Cytotechnology **21:** 45–59, 1996.

Death rate in a small air-lift loop reactor of vero cells grown on solid microcarriers and in macroporous microcarriers

D.E. Martens[1], E.A.A. Nollen[2], M. Hardeveld[3], C.A.M. van der Velden-de Groot[3], C.D. de Gooijer[1], E.C. Beuvery[3] & J. Tramper[1]

[1] *Department of Food Science, Food and Bioengeneering Group, Agricultural University, Bomenweg 2, 6703 HD Wageningen, The Netherlands;* [2] *present adress: Department of Radiobiology, University of Groningen, Bloemsingel 1, Groningen, The Netherlands;* [3] *Laboratory of Inactivated Viral Vaccines, National Institute of Public Health and Environmental Protection, P.O. Box 1, 3720 BA Bilthoven, The Netherlands*

Received 19 December 1995; accepted 3 April 1996

Key words: air lift, macroporous, microcarrier, shear, sparging, Vero cell

Abstract

The death rate of Vero cells grown on Cytodex-3 microcarriers was studied as a function of the gas flow rate in a small air-lift loop reactor. The death rate may be described by first-order death-rate kinetics. The first-order death-rate constant as calculated from the decrease in viable cells, the increase in dead cells and the increase in LDH activity is linear proportional to the gas flow rate, with a specific hypothetical killing volume in which all cells are killed of about $2 \cdot 10^{-3}$ m^3 liquid per m^3 of air bubbles. In addition, an experiment was conducted in the same air-lift reactor with Vero cells grown inside porous Asahi microcarriers. The specific hypothetical killing volume calculated from this experiment has a value of $3 \cdot 10^{-4}$ m^3 liquid per m^3 of air bubbles, which shows that the porous microcarriers were at least in part able to protect the cells against the detrimental hydrodynamic forces generated by the bubbles.

Introduction

In small-scale microcarrier cultures of animal cells gentle agitation is required to keep the microcarriers from settling and to provide a homegeneous environment. At larger scales, more vigorous agitation is needed in order to enhance the mass transfer rate of nutrients and toxic metabolites. Besides more vigorous, agitation, sparging might be required to increase the oxygen transfer rate. However, hydrodynamic forces associated with agitation and sparging are detrimental to animal cells, which has led to the design of bubble-free-aeration reactors (Henzler, 1993). Although these reactors have been operated successfully, they are also limited in their application scale and usually have a more complex design than the standard reactors, like the stirred tank, bubble-column and air-lift loop reactor (Henzler, 1993). At larger scales the use of bubble-column and air-lift loop reactors might become feasible. These reactors have, even at larger scales, good oxygen and mass transfer characteristics, a relative simple design through the absence of mechanical agitation and the hydrodynamic behavior and mass transfer characteristics are well documented in literature (Chisti, 1889). However, as stated, the presence of air bubbles causes cell damage and death.

The effect of hydrodynamic forces generated by air bubbles on suspension cells has been extensively studied (Bavarian *et al.*, 1991; Chalmers and Bavarian, 1991; Cherry and Hulle, 1992; Handa-Corrigan *et al.*, 1989; Jöbses *et al.*, 1991; Jordan *et al.*, 1994; Kunas and Papoutsakis, 1990; Martens *et al.*, 1992; Martens *et al.*, 1993; van der Pol *et al.*, 1990; Tramper *et al.*, 1986; Tramper *et al.*, 1988; Trinh *et al.*, 1994) as well as the effect of agitation on microcarrier cultures (Cherry and Papoutsakis, 1986; Croughan *et al.*, 1989; Croughan and Wang, 1990; Lakothia and Papoutsakis, 1992) and has been reviewed by Papoutsakis (1991). Nonetheless, not much is known about the detrimental effects of air bubbles on microcarrier cultures. This is

mainly because the upward moving air bubbles cause aggregation of the microcarriers and accumulation of the microcarriers at the air-medium interface making the application of microcarriers in bubble-column and air-lift reactors impractical (Papoutsakis, 1991).

The problems of microcarrier aggregation and accumulation at the air-medium interface could be overcome in this study by reducing the foam formation through the careful addition of antifoam, which made it possible to study the effect of sparging on microcarrier cultures. A careful study of the death rate in air-lift and bubble-column ractors as a function of process and reactor parameters, like the gas flow rate and the height and diameter of the reactor, might lead to a minimization of cell death in these reacors and to an optimal reactor design. Cell damage might also be reduced through the addition of shear-protective agents like pluronics. In this paper the death rate of Vero cells grown on Cytodex-3 microcarriers in a small air-lift loop reactor is studied at varying gas flow rates. In addition, an experiment was conducted with Vero cells grown inside porous Asahi microcarries, to study if these microcarriers can protect the cells from the detrimental hydrodynamic forces caused by sparging.

Material and methods

Cell culture

For the shear experiments at varying gas flow rates Vero cells were cultured on Cytodex-3 microcarriers (Pharmacia, Uppsala, Zweden) at a concentration of 2.5 g dm^{-3}. Cultures were conducted in spinner flasks (Techne, Cambridge, UK) with a working volume of 0.25 dm^3 at a temperature of 37 °C and an agitation rate of 25 rpm. The medium was Iscove's modified Dulbecco's medium (Gibco laboratories, Paisley, Scotland) supplemented with antibiotics (35000 $U.dm^{-3}$ polymyxin, 1400 $U.dm^{-3}$ neomycin and 7500 $U.dm^{-3}$ streptomycin) and 5% (v/v) heat-inactivated (30 minutes 56 °C) fetal-calf serum (FCS) (Sanbio, Uden, the Netherlands). A mixture of air/5% CO_2 was blown over the surface of the cultures twice daily to maintain the pH above 7.0 and the dissolved oxygen concentration above zero. If the microcarriers were fully grown with cells, which was always after about 95 hours, they were used for the shear experiments.

For the experiments with the porous microcarriers Vero cells were grown in the same medium inside Asahi microcarriers (Asahi Chemical Industry, Osaka, Japan) at a concentration of 1 g dm^{-3}. In parallel to these cultures reference cultures were conducted with Vero cells on Cytodex-3 microcarriers. In order to have the same available surface for growth, the concentration of Cytodex-3 microcarriers was 5 $g.dm^{-3}$ in these cultures. Samples for shear experiments were taken after 50 and 95 hours of culture.

Shear sensitivity

The shear sensitivity of the cells was determined in a small air-lift reactor with an internal loop. For the experiments 65 cm^3 samples were taken from spinner-flask cultures of which 45 cm^3 was put directly in the air lift. The other 20 cm^3 was centrifuged and the cell-free supernatant was used during the shear experiment as will be described. The air lift was thermostated at 37 °C by a water jacket. Air containing 5% CO_2 was sparged into the inner tube through a nozzle with a diameter of 0.001 m. The flow rates were controlled by a Brooks rotameter and measured exactly after each experiment.

The inner diameter of the draught tube was 0.012 m, the fluid height 0.07 m and the inner diameter of the outer tube was 0.03 m. Experiments were carried out in duplo at gas flow rates of $0.7 \cdot 10^{-6}$, $1.1 \cdot 10^{-6}$, $2.2 \cdot 10^{-6}$, $5\ 10^{-6}$ $m^3\ s^{-1}$. During the experiments 1% (v/v) anti-foam Silicone B (Baker, Deventer, NL) solution in phosphate buffered saline (PBS) was added every time foaming occurred. The total amount of anti-foam added was smaller than 0.1% (v/v) for the experiments at the lower gas flows. For the experiments conducted at a gas flow rate of $5 \cdot 10^{-6}$ and $8.4 \cdot 10^{-6}$ $m^3\ s^{-1}$ this was 0.2% (v/v) and 0.3% (v/v), respectively. Samples were sheared for a period of 3 hours and every half hour an amount of 3 or 4 cm^3 was withdrawn for measurement of the viable-cell concentration, dead-cell concentration and LDH activity. If the liquid volume of the air lift dropped below 45 cm^3 due to sampling, 3 or 4 cm^3 of the previously obtained cell-free medium was added depending on the sample volume. If, due to the addition of antifoam, the volume was higher than 45 cm^3 after sampling, no medium was added. As a consequence of the addition of antifoam and medium the contents of the air lift were diluted resulting in lower cell concentrations. Furthermore, in the case of medium addition also small amounts of LDH activity and serum, which were originally present in the spinner culture, were added. Using the amount of added antifoam and medium and the volume of the sample, the measured concentrations were calculated back to

theoretical concentrations that would have been actual if no additions or withdrawals had taken place.

Cell counts

Cells were counted using a Fuchs-Rosenthal hemacytometer. Cells in suspension were counted using the exclusion of trypan blue (1% w/v) to discriminate between viable and dead cells. The concentration of attached cells was determined by incubating the carriers with a solution of crystal violet (1 g dm^{-3}) in citric acid (0.1 M). The error in the cell count was about 10%.

Lactate-dehydrogenase (LDH) activity

Lactate-dehydrogenase activity was determined by an enzymatic assay (Baker, Deventer, NL).

Photography

Photographs were taken of cells on microcarriers stained with haematoxylon (1 g dm^{-3} at different stages during a shear experiment using an Minolta MPS camera with a Ektachrome (Kodak) film placed on a Leitz Wetzlar microscope.

Determination methods death-rate constant

Three methods, based on the viable-cell, dead-cell, and LDH concentrations, respectively, were used to determine the first-order death-rate constant. The first method uses the decrease in the viable-cell concentration and the associated first-order death-rate constant may be calculated according to:

$$-Ln\left(\frac{C_{x_v}(t)}{C_{x_v}(0)}\right) = k_{dv}t \qquad (1)$$

where $C_{xv}(t)$ *and* $C_{xv}(O)$ are the viable-cell concentrations (cells m^{-3}) at time t=t *(s)* and t=O *(s)*, respectively, and k_{dv} is the viable-cell-based first-order death-rate constant (s^{-1}).

The second method uses the increase in the dead-cell concentration and assumes that no lysis of cells occurs. This first-order death-rate constant may be calculated according to:

$$-Ln\left(\frac{C_{x_v}(0) - C_{x_d}(t) + C_{x_d}(0)}{C_{x_v}(0)}\right) = k_{dd}t \qquad (2)$$

where $C_{xd}(t)$ and $C_{xd}(O)$ are the dead-cell concentrations (Cells m^{-3}) at time t=t *(s)* and t=O *(s)*, respectively, and k_{dd} is the dead-cell-based first-oder death-rate constant (s^{-1}).

The third method uses the increase in the LDH activity and assumes that a constant amount of LDH activity is released per dead cell formed. The pertinent first-order death-rate constant is calculated according to:

$$-Ln\left(\frac{C_{LDH}(\infty) - C_{LDH}(t)}{C_{LDH}(\infty) - C_{LDH}(0)}\right) = k_{dl}t \qquad (3)$$

where $C_{LDH}(\infty)$ is the maximum attainable LDH activity if all cells are killed (U m^{-3}), $C_{LDH}(t)$ and $C_{LDH}(O)$ are the LDH activities (U m^{-3}) at time t=t *(s)* and t=O *(s)*, respectively, and k_{dl} is the LDH-based first-order death-rate constant (s^{-1}). The maximum attainable amount of LDH activity is calculated from the LDH activity released per dead cell formed, Y_{LDH} $(U.cell^{-1})$, and from the viable-cell concentration and LDH activity at the start of the experiment according to:

$$C_{LDH}(\infty) = Y_{LDH}C_{X_v}(0) + C_{LDH}(0) \qquad (4)$$

Since small variations in the amount of LDH activity per cell exist between the experiments, the value of Y_{LDH} used is not the average value of all experiments but is calculated for each individual shear experiment.

As will be shown, large variations occur in the total- and viable-cell concentration due to difficulties in taking a representative sample of microcarriers. As can be seen in equation 1, 2, 3, and 4 an error in the concentration of viable cells at time zero (C_{xv}(O)) enlarges the error in each datum point and consequently causes an increase in the error in the calculated first-order death-rate constant. Taking more samples per datum point would result in a too large withdrawal of medium with microcarriers. Therefore, a more reliable value for the concentration of viable cells at the start of the experiment is obtained by calculating it from the average total-cell concentration at all datum points and the dead-cell concentration at the start of the experiment according to:

$$C_{X_v}(0) = \left\{\frac{1}{7}\sum_{n=1}^{7} C_{X_t}(t_n)\right\} - C_{X_d}(0) \qquad (5)$$

where $C_{xt}(t_n)$ is the total-cell concentration (cell m^{-3}) at time t=t_n.

For the measurements of the LDH activity and the dead-cell concentration the problem of taking a representative sample does not exist and thus the measured

values are more reliable. However, for the calculation of the LDH- and dead-cell-based death-rate constant an extra substraction has to be executed as compared to the calculation of the viable-cell-based death-rate constant. Especially at high gas flow rates when the LDH activities and dead-cell concentrations become large and the result of the substraction is small, this leads to large confidence intervals for the first-order death-rate constants. A clear advantage of using the LDH activity is that it requires only very small (200 μl) sample volumes. This makes it possible to take more samples during the experiment without diluting the air-lift contents. In addition, this method also accounts for cell lysis. If cell lysis occurs, the value of Y_{LDH} may be obtained by lysing all cells at the end of a shear experiment. Thus, the three calculation methods are related through a cell and LDH balance and provided that no lysis of cells occurs and that a constant amount of LDH is released upon cell death they should give the same values for the death-rate constant. The difference between the three medhods lies in the accuracy with which these values can be determined.

Results and discussion

Growth curves

Figure 1 shows three typical growth curves for Vero cells on Cytodex-3 microcarriers (2.5 g dm^{-3}). By plotting the logarithm of the viable-cell concentration against time, the specific growth rate may be determined from the slope of the least-square regression line through the datum points measured during the exponential growth phase. The thus obtained average growth rate in the exponential phase was 0.025 h^{-1} and the final cell densities were about $1.5 \cdot 10^6$ cells. cm^{-3}. Differences between samples in terms of physiological state of the cells, medium composition and number of cells per carrier, are minimized by conducting all batch cultures in the same way and by taking the samples for the shear experiments always after 95 hours of culture, when the microcarriers were totally covered with cells. Furthermore, duplo or even triplo shear experiments were conducted with cells taken from different batch cultures as is shown in Table 1.

LDH and cell concentrations during a shear experiment.

Figure 2 shows the LDH activities and the viable-, dead- and total-cell concentrations as a function of exposure time in the small air-lift reactor at the lowest (2A, $0.7 \cdot 10^{-6}$ m^3 s^{-1}), an intermediate (2B, $5.0 \cdot 10^{-6}$ m^3 s^{-1}), and the highest (2C, $8.4 \cdot 10^{-6}$ m^3 s^{-1}) gas flow rate. For the other three gas flow rates comparable figures are obtained. The confidence limits represent the

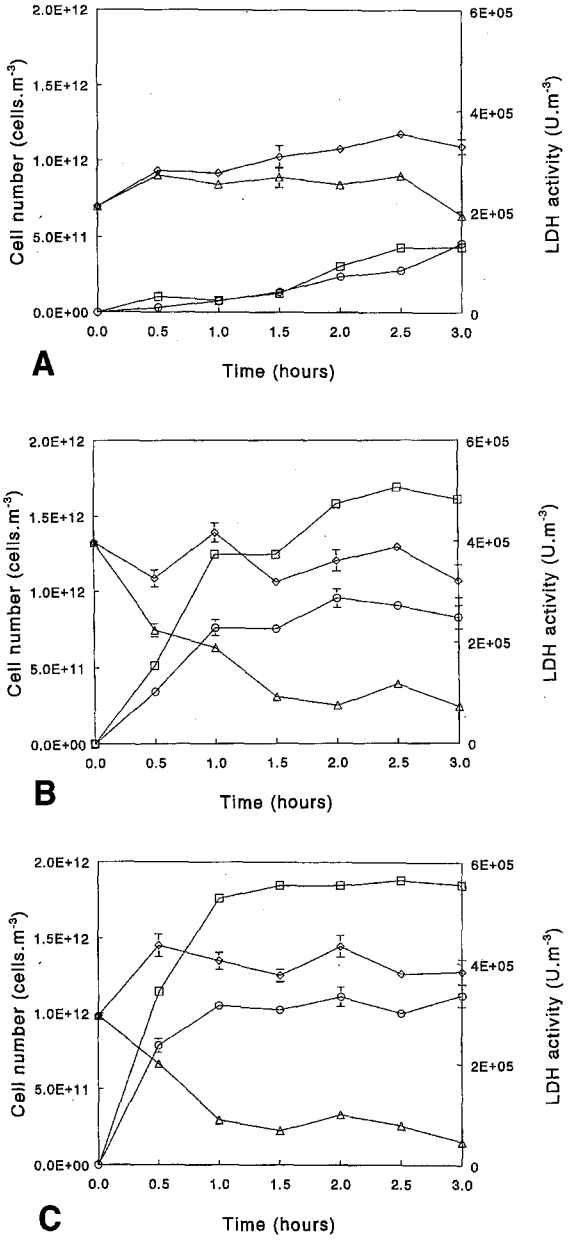

Figure 2. Viable-, dead- and total-cell numbers and LDH activities for shear experiments conducted at gas flow rates of $0.7\ 10^{-6}$ m^3 s^{-1} (A), $5.0 \cdot 10^{-6}$ m^3 s^{-1} (B) and $8.4 \cdot 10^{-6}$ m^3 s^{-1} (C). ◇ Total cells, △ Viable cells, ○ Dead cells, □ LDH activity.

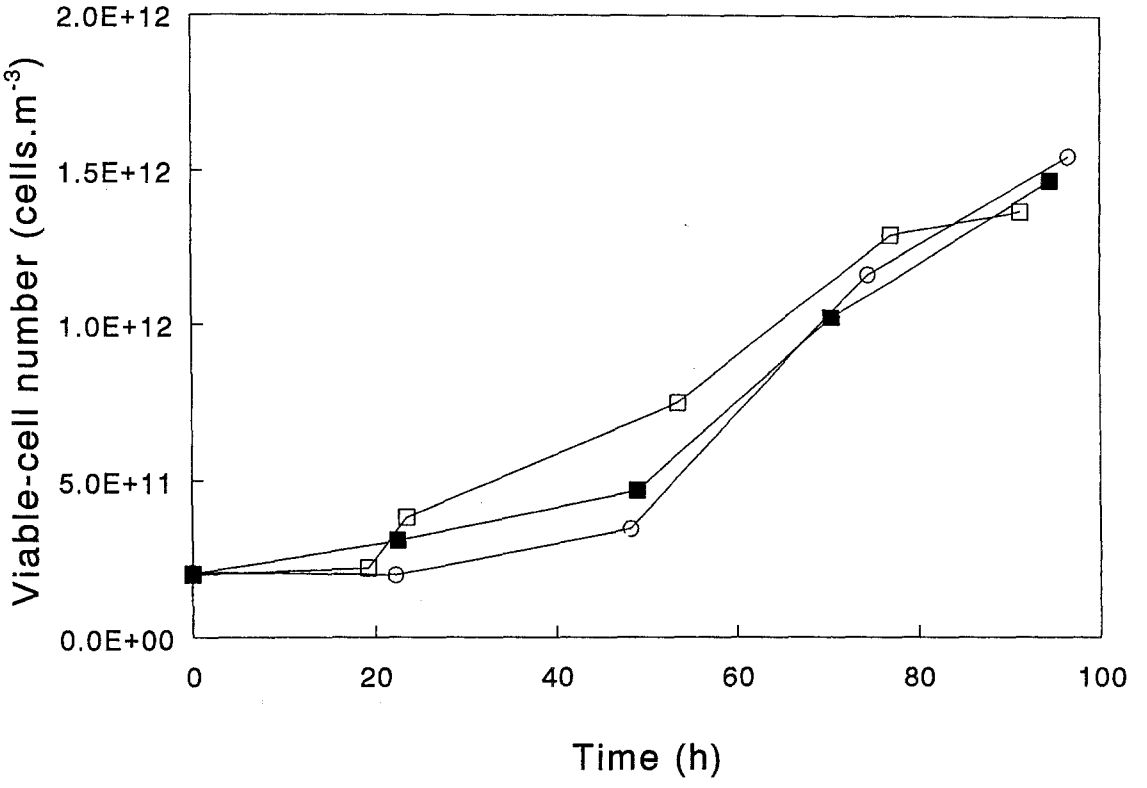

Figure 1. Growth curves of Vero cells grown on Cytodex-3 microcarriers (2.5 g dm^{-3}). Different symbols denote separate batch cultures conducted at identical conditions.

variation of the cell counts and LDH activities within a sample and not between the samples. At the lowest gas flow rate of $0.7 \cdot 10^{-6}$ m^3 s^{-1} a small amount of growth seems to occur when looking at the total-cell concentration. At higher gas flow rates no significant increase in the total-cell concentration occurs. For the experiment at the highest gas flow rate (Figure 2C) a large increase in the total cell density occurs at the second sample (t=0.5 h). Since the total cell density remains constant thereafter, this is probably due to an error in the sampling at t=0 h, resulting in a too low total-cell concentration at this point. The on average constant total-cell concentration at gas flow rates higher than $0.7 \cdot 10^{-6}$ m^3 s^{-1} may be the result of the growth rate being equal to the rate of cell lysis due to shear forces. However, if cell lysis occurs it may be expected to increase at higher gas flow rates. Since the growth rate is likely to have more or less the same value in all shear experiments and will always be smaller than 0.025 h^{-1}, this would lead to a decrease in the total-cell concentration at high gas flow rates, which is not seen. Thus, cell growth and the amount of cell lysis may assumed to be negligible.

LDH activity per dead cell formed

In Figure 3 the LDH activity is plotted as a function of the concentration of dead cells in suspension for all shear experiments. In addition, the least-square regression line and the 95% prediction intervals are shown. All cells in suspension were dead, while the amount of dead cells still attached to microcarriers was negligible. As can be seen the LDH activity is linear proportional to the dead-cell concentration. With the amount of cell lysis being negligible, the amount of LDH activity released per dead cell formed, Y_{LDH} (U.$cell^{-1}$), is equal to the slope of the least-square regression line through the datum points, which has a value of $4.1 \pm 0.4 \cdot 10^{-7}$ U.$cell^{-1}$. This is of the same order of magnitude as the values found by Legrand *et al.* (1992) of $4\text{–}5.5 \cdot 10^{-7}$ U.$cell^{-1}$ and by Gardner *et al.* (1990) of $2.85 \cdot 10^{-7}$ U.$cell^{-1}$. Geaugey (1990) showed that the LDH activity depended on the physiological state of the cell with regard to the oxygen tension. They found

Table 1. First-order death-rate constants with 95% confidence intervals for the three determination methods at varying gas flow rates. The number between parentheses in the first column indicates the batch culture from which the sample was taken

Experiment	F (10^{-6} m^3 s^{-1})	V (10^{-6} m^{-3})	$K_{d,viab}$ (10^{-5} s^{-1})	$k_{d,dead}$ (10^{-5} s^{-1})	$k_{d,LDH}$ (10^{-5} s^{-1})
Flow 1A (2)	0.68	56.6	4.2±4.0	6.4±2.6	6.7±1.1
Flow 1B (8)	0.70	46.0	2.5±2.9	5.0±2.1	3.4±1.4
Flow 1C (5)	0.65	50.6	3.5±4.1	5.5±3.2	5.0±1.6
Flow 2A (1)	1.17	50.1	8.4±5.0	7.7±2.3	5.7±1.6
Flow 2B (5)	1.15	42.5	6.8±4.6	11.9±6.3	9.7±3.5
Flow 3A (2)	2.22	50.8	12.1±4.2	10.8±1.4	9.9±1.8
Flow 3B (7)	2.30	43.9	11.4±2.7	11.1±7.3	12.9±1.7
Flow 3C (6)	2.25	47.2	12.5±4.5	10.3±5.8	10.8±2.6
Flow 4A (3)	5.09	48.3	22.6±9.1	21.0±9.1	22.3±10.1
Flow 4B (8)	5.10	49.9	22.2±5.7	22.0±15.5	25.5±7.8
Flow 5A (4)	8.35	52.3	32.6±18.8	32.4±39.2	38.3±20.6
Flow 5B (8)	8.51	51.6	33.2±7.1	45.2±52.1	50.9±26.7
Antifoam (9)	0.68	45.6	5.9±2.7	9.4±2.3	10.6±10.1

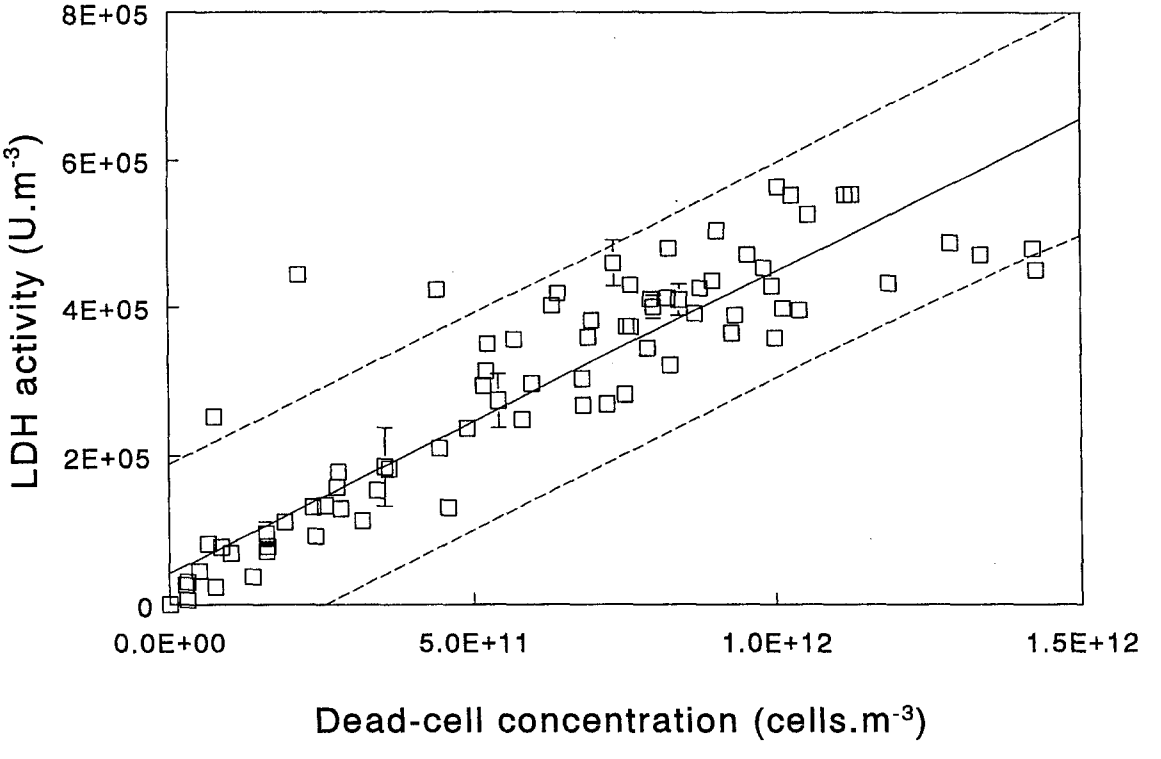

Figure 3. LDH activities □, least-square regression line (solid line) and 95% prediction intervals (dashed lines) as a function of the dead-cell concentration for all shear experiments.

a value of $2.7 \cdot 10^{-7}$ U.cell^{-1} at a dissolved oxygen tension of 30% and a value of 6.2 10^{-7} U.cell^{-1} for a dissolved oxygen tension of 1%. Here all cell cultures were conducted in the same way and thus probably have on average the same dissolved oxygen tension. As can be seen in Figure 3 no large differences in the intracellular LDH content exist between the cell cultures indicating that the physiological state of the cells is more or less equal with respect to the LDH content.

First-order death-rate constant as a function of the gas flow rate.

Shear experiments

In Figure 4 the logarithm of the relative decrease in the viable-cell concentration (eq. 1) is plotted as a function of time for a single series of shear experiments. For the duplo series of experiments comparable figures are obtained. Also for the dead-cell (eq. 2) and LDH (eq. 3) data comparable plots are obtained, where only the confidence intervals for the datum points are larger. The gas flow rates, average volume during the experiment and the calculated death-rate constants for the three different determination methods are given in Table 1 for all experiments. In general the cell death can be described by first-order death-rate kinetics. Only for the dead-cell-based data (eq. 2) of the experiments at the lowest gas flow rates (1A, 1B, 1C, 2A, and 2B) and the LDH-based data (eq. 3) of experiment 1C and 2B a small increase is seen in the death rate during the experiment (data not shown). Since this is only seen at the two lowest gas flow rates, it may be due to the occurrence of a small amount of cell growth during the experiment. For the experiments at the two highest gas flow rates almost all cells were killed after 1.5 to 2 hours, and the experiments were stopped then.

Since cell lysis is negligible and the amount of LDH activity released per dead cell formed is more or less constant (Figure 3), the three different methods should give the same values for the first-order death-rate constant, which is indeed the case (Table 1). In addition, there are no significant differences between duplo and triplo measurements, indicating that with respect to shear sensitivity the physiological state of the cells in the different experiments was the same. In the experiments conducted at the highest as flow rate (Flow 5B), the dead-cell-based and LDH-based death-rate constant deviate quite much from the viable-cell-based value and from their values in the duplo experiment (Flow 5A). However, as expected, the dead-cell-, and LDH-based death-rate constants become quite unreliable at higher gas flow rates and the deviations are not significant. When looking at the full range of studied gas flow rates the viable-cell-based method has about the same reliability as the other methods at lower gas flow rates and is more reliable at the higher gas flow rates. As shown for the viable-cell-based method in Figure 5, the first-order death-rate constant is linearly proportional to the gas flow rate.

Influence of antifoam

During the sparging experiments small amounts of antifoam were added whenever foam formation occurred. At low gas flow rates (below $5.0 \cdot 10^{-6}$ m^{-3} s^{-1}) less than 0.1% antifoam was added. According to van der Pol *et al.* (1993) this would still increase the death rate by a factor two. However, they added all the antifoam at the start of the experiment, while here it was added only if foaming started to occur. Additionally, in parallel to the air-lift experiment conducted at a gas flow rate of $2.2 \cdot 10^{-6}$ m^3 s^{-1} a spinner flask experiment was conducted. For this experiment, microcarriers totally covered with cells and from the same origin as the ones used in the air-lift experiment, were put in a small spinner flask agitated at 100 rpm. During a period of three hours every time antifoam was added to the air lift, an equal amount was added to the spinner flask. No cell death occurred in the spinner flask showing that antifoam in itself was not responsible for cell death. To test if antifoam would render the cells more sensitive to sparging, an air-lift experiment was conducted at a gas flow rate of $0.7 \cdot 10^{-6}$ m^3 s^{-1} to which the same amounts of antifoam were added as in the experiment conducted at a gas flow rate of 8.4 10^{-6} m^3 s^{-1}. The final concentration was 0.3% as compared to a final concentration of 0.05% normal for experiments at this gas flow rate. The results in Figure 6 and Table 1 show a small and insignificant increase in the death-rate constant as compared to the experiment conducted at $0.7 \cdot 10^{-6}$ m^3 s^{-1} with a final antifoam concentration of about 0.05%. This increase is negligible compared to the increase in the death-rate constant caused by the increase in gas flow rate to $8.4 \cdot 10^{-6}$ m^3 s^{-1}. Thus effects of antifoam on the death-rate constant may be neglected. For comparison the death-rate constant of the antifoam experiment is also shown in Figure 5 (filled symbol).

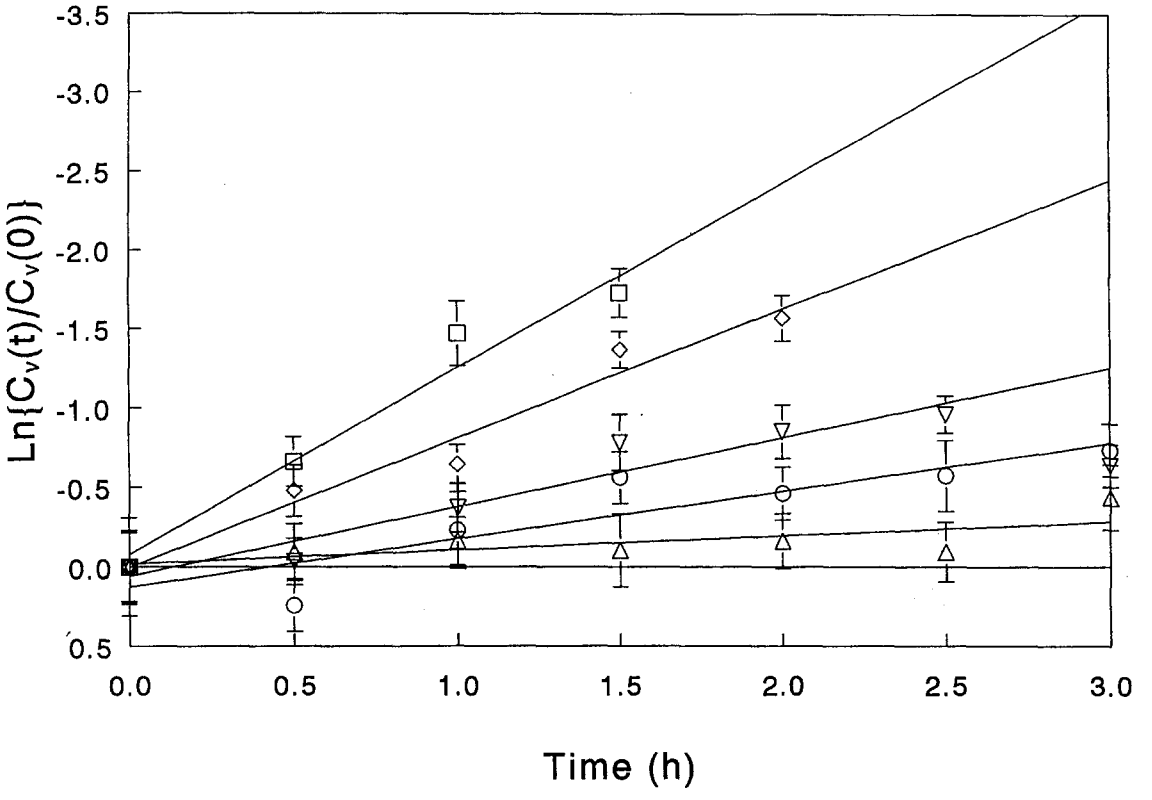

Figure 4. Logarithmic plot for the determination of the first-order death-rate constant according to the decrease in viable-cell concentration (eq. 1). △ $0.7 \cdot 10^{-6}$ m^3 s^{-1}, ○ $1.17 \cdot 10^{-6}$ m^3 s^{-1}, ▽ $2.22 \cdot 10^{-6}$ m^3 s^{-1}, ◇ 5.0 10^{-6} m^3 s^{-1}, □ $8.4 \cdot 10^{-6}$ m^3 s^{-1}.

Specific hypothetical killing volume

To describe the death rate of suspension cells in bubble-column and air-lift reactors the hypothetical killing volume model of Tramper *et al.* (van 't Riet and Tramper 1991) may be used. The model assumes first-order death-rate kinetics and a hypothetical killing volume associated with each air bubble, in which all cells are killed. This results in the following equation for the first-oder death-rate constant, k_d (s^{-1}):

$$k_d = \frac{24FX}{\pi^2 d_b^3 D^2 H} \qquad (6)$$

where F is the gas flow rate (m^3 s^{-1}) d_b is the bubble diameter (m), D is the reactor diameter (m), H is the reactor height (m), and X is the hypothetical killing volume (m^3). Tramper *et al.* (1988) showed that the hypothetical killing volume was proportional to the bubble volume for bubble diameters in the range of $2\text{–}6 \cdot 10^{-3}$ m and thus equation 6 can be simplified to:

$$k_d = \frac{4FX'}{\pi^2 D^2 H} \qquad (7)$$

where X' is the specific hypothetical killing volume (–) being the hypothetical killing volume divided by the volume of the air bubble. Trinh *et al.* (1994) and Jordan *et al.* (1994) relate the hypothetical killing volume to a real volume associated with an air bubble.

The hypothetical killing volume model is used here to describe the death rate of Vero cells immobilized on Cytodex-3 microcarriers in a small air-lift loop reactor as a function of the gas flow rate. By plotting the first-order death-rate constant as a function of the gas flow rate, the specific hypothetical killing volume may be calculated according to equation 7 from the slope of the least-square regression line for all three methods. The line is shown in Figure 5 for the viable-cell-based data. The volume of the samples in the different shear experiments varies between about 43 and 52 cm^3 and an average value obtained from all experiments of 48 cm^3 is used in equation 7. Since no differences existed between the death-rate constants of the three methods no significant differences in specific hypothetical killing are found between the three different

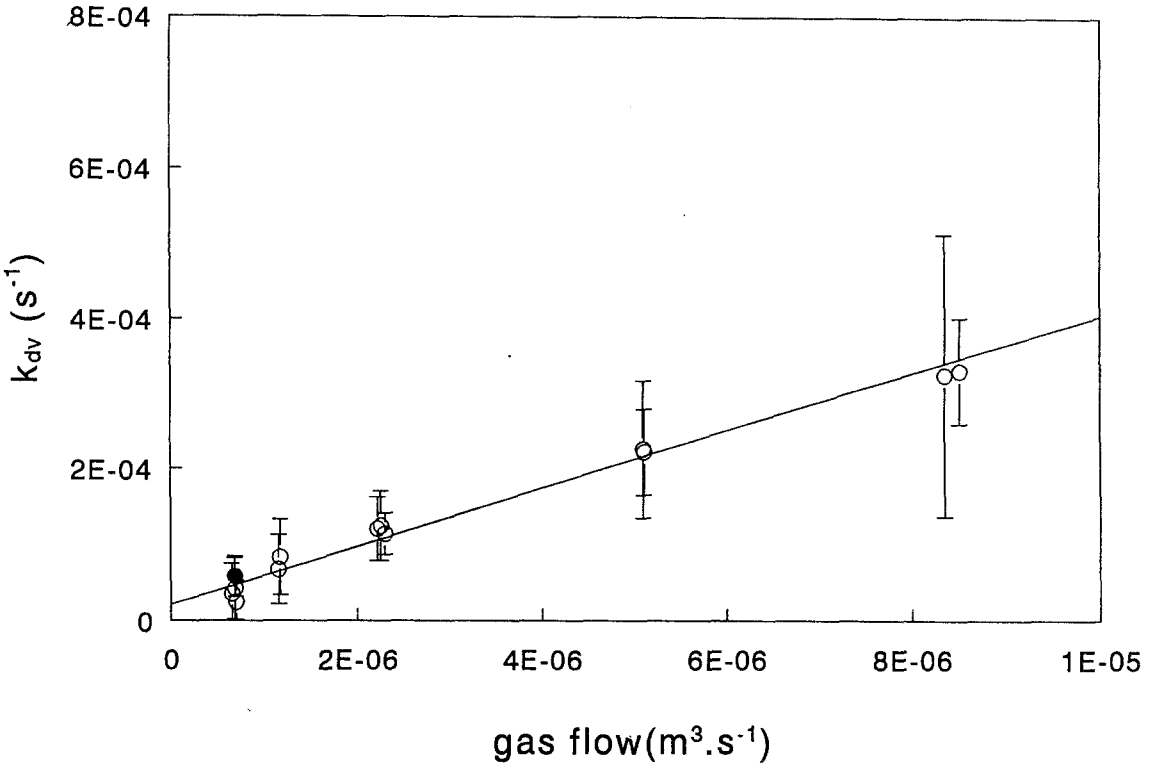

Figure 5. First-order death-rate constant as a function of the gas flow rate calculated on the basis of the decrease in the viable-cll concentration. The filled symbol represents an experiment executed at $0.7 \cdot 10^{-6}$ m^3 s^{-1} with the same amount of antifoam added as in the experiment conducted at $8.4 \cdot 10^{-6}$ m^3 s^{-1}.

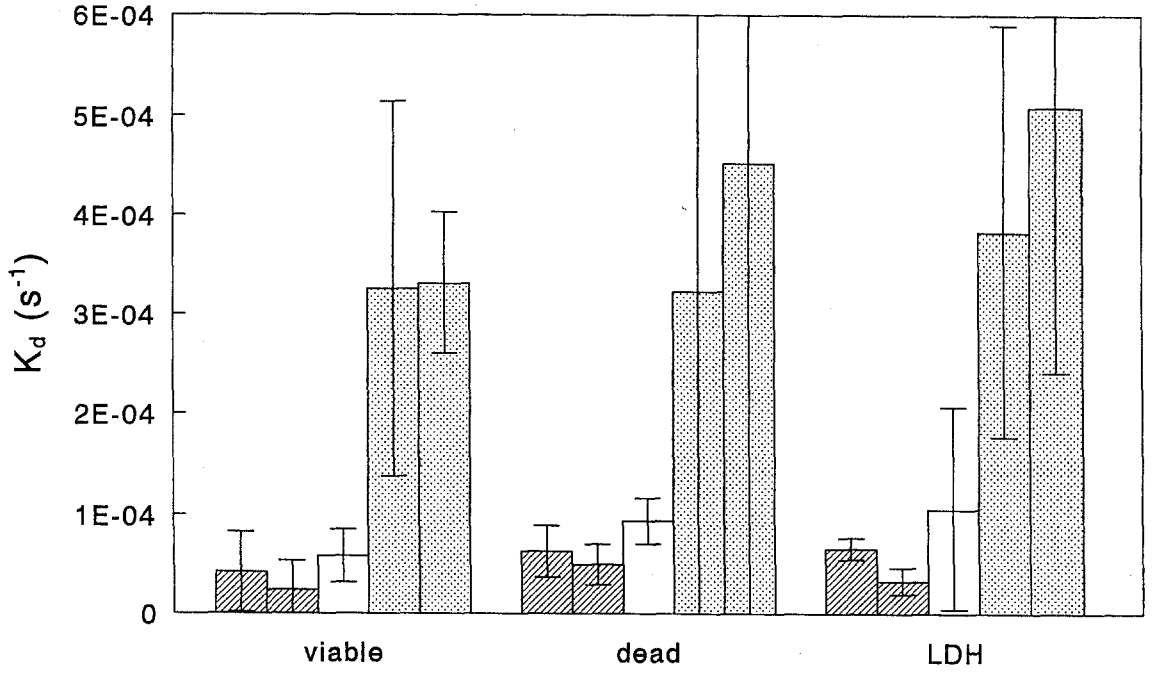

Figure 6. First-order death-rate constants for the antifoam control experiment. Dashed: $F=0.69 \cdot 10^{-6}$ m^3 s^{-1}, [AF]=0.05%, Blank: Antifoam control experiment $F=0.69 \cdot 10^{-6}$ m^3 s^{-1}, [AF]=0.3%, Dotted: $f=8.4 \cdot 10^{-6}$ m^3 s^{-1}, [AF]=0.3%.

determination methods. The average value of the specific hypothetical killing volume is $2\pm0.2\cdot10^{-3}$ (-).

Literature values for the specific hypothetical killing volume show a large variation. This is caused by the fact that the specific hypothetical killing volume will depend on the cell line and type, serum concentration (Martens *et al.*, 1992; van der Pol *et al.*, 1990) and growth rate (Martens *et al.*, 1993), which are distinct in the experiments presented by the different authors. For insect cells in bubble columns Tramper *et al.* (1988) found a value of $4\cdot10^{-3}$ at a serum concentration of 10%. For hybridoma cells in bubble columns Jöbses *et al.* (1991) reported a value of $7\cdot10^{-3}$ (1% serum) and van der Pol *et al.* (1990) a value of $9\cdot10^{-3}$ (5% serum). For hybridoma cells in an air-lift reactor a value of $2\cdot10^{-4}$ (5% serum) is found (Martens *et al.*, 1992). Because of the variations in experimental conditions, it is difficult to compare the results, although the value of the specific killing volume for Vero cells on cytodex-3 microcarriers is of the same order of magnitude as the values found for suspension cells.

Summarizing it may be concluded that the death of Vero cells on Cytodex-3 microcarriers in a small air-lift reactor can be described by first-order kinetics and is linear proportional to the gas flow rate.

Photography

Figure 7 shows a series of representative photographs of Vero cells on Cytodex-3 microcarriers after 0, 1, 2, and 3 hours of shearing at a gas flow rate of $0.7\cdot10^{-6}$ $m^3\ s^{-1}$. In all experiments clear regions could be discerned, where whole groups of cells were removed. Furthermore, in all experiments at higher gas flow rates clusters of two or three microcarriers were seen towards the end of an experiment (data not shown). The clusters were held together by cells, which seemed to pile up in the contact regions and were marked as dead by trypan-blue staining.

Death rate of Vero cells immobilized in porous Asahi carriers

One of the advantages of using porous microcarriers rather than solid microcarriers is that the matrix of the porous microcarrier might protect the cells against hydrodynamic forces. Bugarski *et al.* (1989) successfully cultured hybridomas inside alginate beads and microcapsules in an air-lift reactor with an external loop. Shiragami *et al.* (1993) showed that porous Cultisphere microcarriers could protect CHO cells against the detrimental effect of air bubbles. Additionally, porous microcarriers have a larger available surface for growth and thus support higher cell concentrations at the same microcarrier loading. However, growth inside the porous microcarrier may be limited by the diffusion rate of nutrients into the microcarrier and toxic metabolites out of the microcarrier (Cahn, 1990). Further, it may be difficult to count the amount of viable cells due to difficulties in extracting the cells from the inside of the microcarrier without killing them (Cahn, 1990). An experiment was executed to see if a porous microcarrier could indeed protect cells from hydrodynamic forces generated by air bubbles. For this the death rate in the small air-lift reactor was compared for Vero cells immobilized inside porous Asahi microcarriers and Vero cells immobilized on Cytodex-3 microcarriers. The protective effect is quantified by calculating the specific hypothetical killing volume.

Cells for the shear experiments were grown on Cytodex-3 and inside Asahi microcarriers in spinner flasks. To obtain an equal available surface for growth in both systems, the microcarrier concentration was 5 g dm^{-3} for Cytodex-3 and 1 g dm^{-3} for the Asahi microcarriers. The growth rate was determined as described and had a value of 0.022 h^{-1} for cells grown on Cytodex-3 microcarriers and 0.018 h^{-1} for cells grown inside Asahi microcarriers. Two samples at 50 and 95 hours of culture, respectively were taken for shear experiments. The gas flow rate during the shear measurements in the air lift was $5.0\cdot10^{-6}$ $m^3\ s^{-1}$. Experiments for cells grown on Cytodex-3 microcarriers were done in duplo. The death-rate constants with cells obtained at 50 and 95 hours of culture are shown in Figure 8 and Table 2. For comparison, the death-rate constants for Vero cells on Cytodex-3 microcarriers at a concentration of 2.5 g fm^{-3} and the same gas flow rate are also given. As can be seen there is no significant difference between the death-rate constants of cells after 50 and 95 hours of culture. The rate constant is significantly smaller for cells inside Asahi microcarriers as compared to cells on Cytodex-3 microcarriers (5 g dm^{-3}) for both sampling times. Since samples are taken at different growth stages of the culture, the reduction in the death rate cannot be explained by a difference in growth state of the cells. Furthermore, the specific hypothetical killing volume calculated from the first–order death-rate constants for Vero cells inside Asahi microcarriers is $3\cdot10^{-4}$ m^3 of air bubbles, which is substantial smaller than the value of $2\cdot10^{-3}$ found for Vero cells on Cytodex-3 microcarriers (2.5 g dm^{-3}). These results form a clear indi-

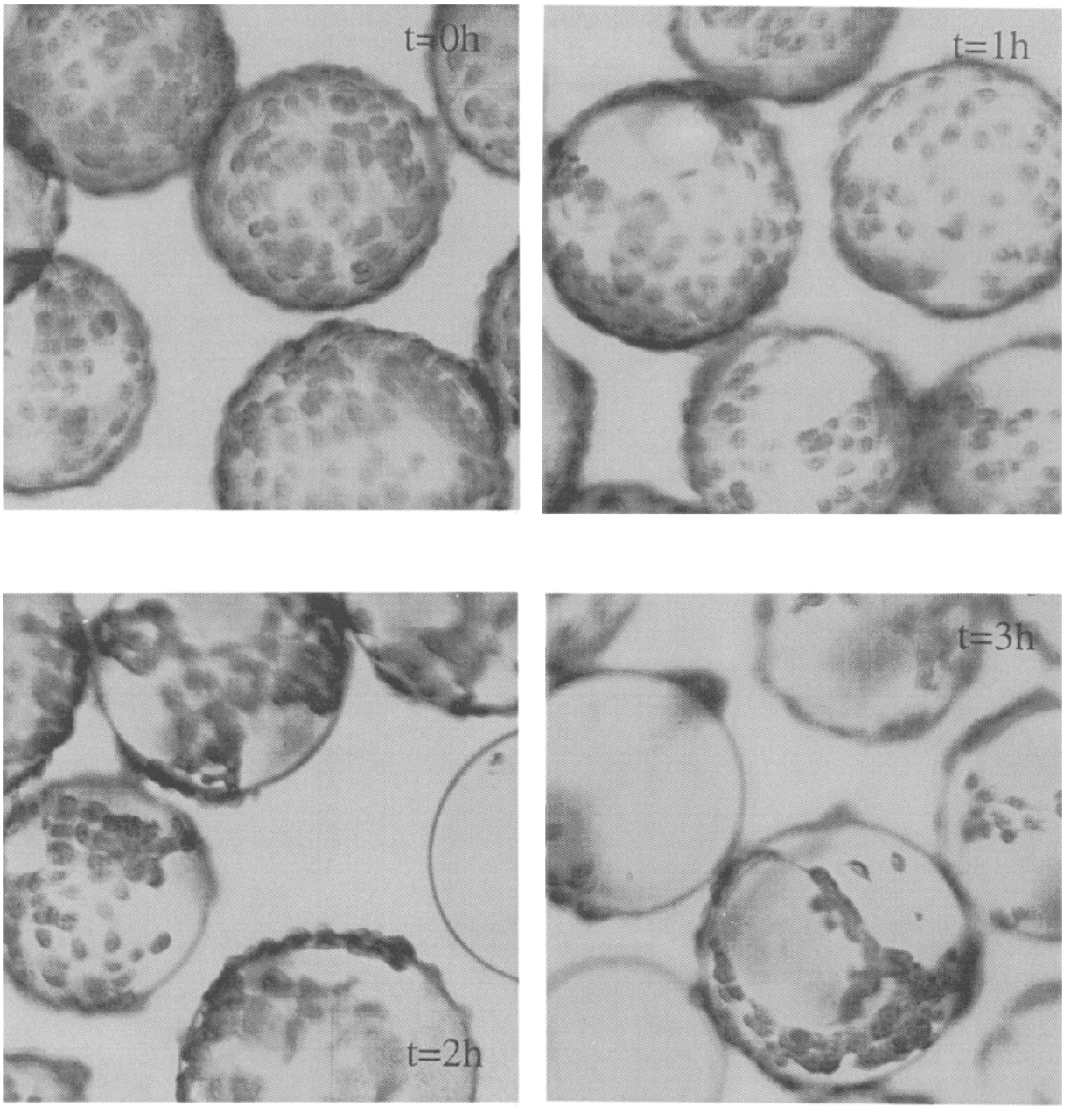

Figure 7. Photographs of Vero cells on Cytodex-3 microcarriers after 0, 1, 2 and 3 hours of shearing in the air-lift reactor at a gas flow rate of $0.7 \cdot 10^{-6}$ m^3 s^{-1}.

cation that the porous Asahi microcarriers protect the cells against hydrodynamic forces. Since the death rate Vero cells inside Asahi microcarriers still exceeds zero, the protection is only partial. Probably cells growing on the periphery of the microcarriers still may be killed by the air bubbles. Shiragami *et al.* (1993) also found that the protection of CHO cells in porous Cultisphere microcarriers was only partial, with cells on the periphery of the microcarrier being especially susceptible to mechanical damage. Nikolai and Hu (1992) found that no growth of Vero cells on Cultisphere microcarriers occurred at agitation rates just high enough to keep the microcarriers from settling. All the cells died and were found in the exterior region of the microcarrier. In a sta-

Table 2. First-order death-rate constants and 95% confidence intervals determined from the decrease in viable cells for cells grown on Cytodex-3 and in Asahi microcarriers. For Asahi and Cytodex-3 (5 g dm^{-3}) microcarriers the death-rate constant was determined after cells were cultured in spinner flasks for 50 hours and 95 hours. For cells grown on Cytodex-3 microcarriers (2.5 g dm^{-3}) the death-rate constant was determined after 95 hours of culture only (These are the same data as presented in Table 1)

Experiment	F (10^{-6} m^3 s^{-1})	V (10^{-6} m^{-3})	k_{dv} (50 h) (10^{-5} s^{-1})	k_{dv} (95 h) 10^{-5} s^{-1})
Cytodex (5 g dm^{-3})	5.0	47.7	17.5±5.6	15.1±2.7
Cytodex (5 g dm^{-3})	5.8	47.8	14.8±10.0	14.4±5.7
Asahi (1 g dm^{-3})	5.0	47.9	2.5±2.2	3.7±3.6
Cytodex Flow 4A (2.5 g dm^{-3})	5.1	48.3	(-)	22.3±9.1
Cytodex Flow 4B (2.5 g dm^{-3})	5.1	49.9	(-)	22.2±8.7

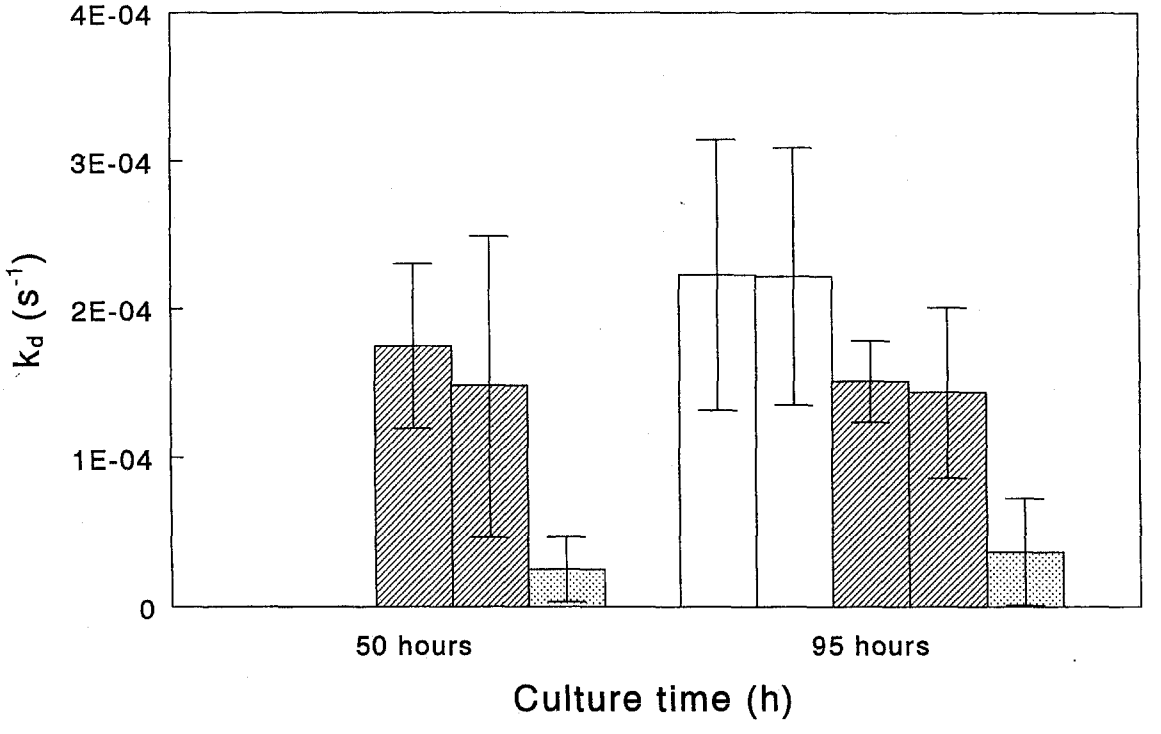

Figure 8. First-order death-rate constants for Vero cells grown on Cytodex-3 microcarriers at 2.5 g dm^{-3} (blank) and 5 g dm^{-3} (dashed) and Vero cells grown in Asahi microcarriers at 1 g dm^{-3} (dotted). Experiments with Cytodex-3 microcarriers were all done in duplicate. Experiments for Cytodex-3 microcarriers (5 g dm^{-3}) and Asahi microcarriers were conducted with samples taken from batch cultures at 50 and 95 hours of culture.

tionary situation cells grew inside the microcarrier cavities. However, they do not report if these cells inside the microcarrier may be protected from hydrodynamic damage. Besides this, differences in microcarrier properties other than the porosity, like for instance the strength with which the cells are adhered to the microcarriers as well as an influence of the microcarrier type on the strength of the cells themselves, may also affect the first-order death-rate constant.

Damage mechanisms

Cells on microcarriers in the air lift may be killed directly by hydrodynamic forces or through the collision of microcarriers (Cherry and Papoutsakis, 1986). At the microcarrier hold up of 0.05 used here, cell death as a consequence of the collision of microcarriers may be neglected (Beverloo and Tramper, 1994). For the shear-related death of cells on microcarriers that, like Vero cells, cannot survive in suspension, the strength of the cell itself as well as the strength with which the cell is attached to the microcarrier is of importance. The tightness of the binding of the cells will depend on the cell line, the microcarrier characteristics, the growth phase of the culture, the medium composition (Lokothia and Papoutsakis, 1992) and the amount of cells per microcarrier. Cell cell contacts may cause the cell to be more tightly bound to the microcarrier and thus be less shear sensitive (Lokothia and Papoutsakis, 1992). Thus removal of a cell may render the neighboring cells more shear sensitive. In addition, hydrodynamic forces affecting a cell may also affect the neighboring cells either directly or through the cell cell contacts. This may explain the observation of the clear spots in Figure 7, where whole groups of cells have been removed from the carrier.

Like for suspension cells (van 't Riet and Tramper, 1991), death of cells on microcarriers due to hydrodynamic forces may occur at three positions in the air lift: i) In the sparger region due to the formation of the bubbles, ii) in the riser and downcomer section due to hydrodynamic forces caused by the rising of the bubbles and the liquid flow, and iii) at the surface due to the bursting of the bubbles.

In the sparger region suspension cells are killed if they come in contact with newly formed bubbles, which are not yet covered with surfactants (Jordan *et al.*, 1994). It seems reasonable to assume that also cells on microcarriers are killed if they come in contact with these bubbles. Since microcarriers totally covered with cells are used, probably a group of cells at a certain spot of the microcarrier will adsorb to the bubble instead of only one cell. This again may explain the observation from the photographs (Figure 7) that it appears that cells are removed in groups from the microcarriers. Apart from this, Murhammer and Goochee (1990) also state that cell death in air-lift reactors may occur in the sparger region and is related to the pressure drop over the orifice.

In case the bubbles are partially saturated with surfactants the cell-bubble contact is not lethal and the cells adsorb to the bubble (Jordan *et al.*, 1994). Adsorption of cells to bubbles has also been shown by Bavarian *et al.* (1994). Microcarriers that have adsorbed to the bubbles may rise with the bubbles to the surface. Although Jordan *et al.* (1994) showed that adsorbed cells could not easily be detached from the bubbles, this may be different for microcarriers, which experience a higher drag force due to their larger size. On the other hand, the contact area between the bubble and the microcarrier may be larger leading to a more tight binding to the bubble. In the case of suspension cells it is shown that the death rate is proportional to the reciprocal reactor height indicating that no cell death occurs in the riser and downcomer section due to the rising of air bubbles or due to the liquid flow (Martens *et al.*, 1992). However, due to the relatively large size of a microcarrier (200 μm) as compared to a suspension cell (20 μm), the liquid velocity a cell on a microcarrier experiences in a laminar flow field will be substantially higher than the liquid velocity a suspension cell experiences in the same flow field. For the case of turbulent flow, occurring in stirred tank and bubble column reactors, the size of the eddies that cause cell death is substantially larger for cells on microcarriers than for suspension cells (Croughan *et al.*, 1989; Lakhotia and Papoutsakis, 1992; O'Connor and Papoutsakis, 1992; Kunas and Papoutsakis, 1990). Thus, cells on microcarriers may be damaged at much lower energy dissipation rates than suspension cells and death of cells on microcarriers in the riser and downcomer section cannot be excluded. Shear experiments in air-lift reactors at varying heights may reveal if events associated with the liquid flow and the rising of air bubbles are detrimental to cells on microcarriers.

At the bubble disengagement zone suspension cells present in the bubble film and near the cavity wall are killed as the bubble ruptures (Chalmers and Bavarian, 1991; Cherry an Hulle, 1992; Trinh *et al.*, 1994). Trinh *et al.* (1994) calculated that a specific killing volume of $2 \cdot 10^{-3}$ would correspond to a film thickness around the air bubble of about 1 to 2 μm. Cherry and Hulle (1992) did the same calculation for a specific killing volume of $4 \cdot 10^{-3}$ and found a value of 5 μm. According to Trinh *et al.* (1994) the thickness of 1 to 2 μm would imply that only cells attached to the bubble are killed. For microcarriers, which are substantially larger than 1 to 2 μm, this would mean that only the cells, which are adsorbed to the air bubble or are very near to it are killed. This also may explain the observation from the photographs (Figure 7) that it appears that cells are removed in groups from the microcarriers.

In conclusion, since forces associated with bubble rupture are high enough to kill suspension cells, it is very likely that they also cause the death of cells immobilized on microcarriers in case these microcarriers are near the bursting bubble. Evidence that larger particles may be near the bursting bubbles is given by Lu *et al.* (1992), who showed that nylon microcapsules varying in size from 20 to 300 μm were ejected in the upward jet formed at bubble break up. Besides death due to bubble break up, additional damage in other parts of the reactor cannot be excluded.

Conclusions

The death rate of vero cells on Cytodex-3 microcarriers can be described by first-order kinetics. The first-order death-rate constant as calculated from the decrease in viable cells, increase in dead cells and increase in LDH activity, is linear proportional to the gas flow rate, which is in accordance with the hypothetical killing volume theory. The specific hypothetical killing volume has a value of $2 \cdot 10^{-3}$ m^3 liquid per m^3 of air bubbles.

Macroporous Asahi microcarriers were able to partly protect the cells against hydrodynamic shear caused by air bubbles. For cells in these microcarriers the hypothetical killing volume was found to be $3 \cdot 10^{-4}$ m^3 liquid per m^3 of air bubbles.

References

Bavarian, F, Fran LS, Chalmers J (1991) Microscopic visualization of insect cell bubble interactions. I: Rising bubbles, air-medium interface, and the foam layer. Biotechnol. Prog 7, 140–150.

Beverloo WA and Tramper J (1994) Intensity of microcarrier collisions in turbulent flow. Bioproc Eng 11, 177–184.

Bugarski B, King GA, Daugulis AJ and Goosen MFA (1989) Performance of an external air-lift bioreactor for the production of monoclonal antibodies by immobilized hybridoma cells. Applied Microbiol Biotechnol 30, 264–269.

Cahn F (1990) Biomaterials aspects of porous microcarriers for animal cell culture. Tibtech 8, 131–136.

Chalmers JJ and Bavarian F (1991) Microscopic visualization of insect cell-bubble interactions. II: The bubble film and bubble rupture. Biotechnol Prog 70, 151–158.

Cherry RS and Papoutsakis ET (1986) Hydrodynamic effects on cells in agitated tissue culture reactors. Bioproc Eng 1, 29–41.

Cherry RS and Hulle CT (1992) Cell death in the films of bursting bubbles. Biotechnol Prog 8, 11–18.

Christi MY (1989) Airlift bioreactors. Elsevier Science Publishers LTD, New York.

Croughan MS, Sayre ES and Wang DIC (1989) Viscous reduction of turbulent damage in animal cell culture. Biotechnol Bioeng 33, 862–872.

Croughan MS, Wang DIC (1990) Reversible removal and hydrodynamic phenomena in CHO microcarrier cultures. Biotechnol Bioeng 38, 316–319.

Gardner AR, Gainer JL and Kirwan DJ (1990) Effects of stirring and sparging on cultured hybrisoma cells. Biotechnol Bioeng 35, 940–947.

Geaugey V, Pascal F, Engasser JM and Marc A (1990) Influence of the culture oxygenation on the release of LDH by hydridoma cells. Biotechnol Techn 4, 257–262.

Handa-Corrigan A, Emery AN and Spier RE (1989) Effect of gas-liquid interfaces on the growth of suspended mammalian cells: mechanisms of cell damage by bubbles. Enzyme Microb Technol 11, 230–235.

Jöbses I, Martens D and Tramper J (1991) Lethal events during gas sparging in animal cell culture. Biotechnol Bioeng 37, 484–490.

Jordan M, Sucker H, Einsele F and Eppenberger HM (1994) Interactions between animal cells and gas bubbles: The influence of serum and pluronic F68 on the physical properties of the bubble surface. Biotechnol Bioeng 43, 446–454.

Kunas KT and Papoutsakis ET (1990) Damage mechanisms of suspended animal cells in agitated bioreactors with and without bubble entrainment. Biotechnol Bioeng 36, 476–483.

Lakhotia S and Papoutsakis ET (1992) Agitation induced cell injury in microcarrier cultures. Protective effect of viscosity is agitation intensity dependent: Experiments and modelling. Biotechnol Bioeng 39, 95–107.

Legrand C, Bour JM, Capiaumont J, Martial A, Marc A, Wudtke M, Kretzmer G, Demangel C, Duval D and Hache J (1992) Lactate dehydrogenase (LDH) activity of the number of dead cells in the medium of cultured eukaryotic cells as marker. J. Biotechnol 25, 231–243.

Lu GZ, Thompson BG and Gray MR (1992) Physical modelling of animal cell damage by hydrodynamic forces in suspension cultures. Biotechnol Bioeng 40, 1277–1281.

Ludwig A, Kretzmer G and Schügerl K (1992) Determination of a 'critical shear stress level' applied to adherent mammalian cells. Enzyme Microb technol 14, 209–213.

Martens DE, Gooijer CD de, Beuvery EC and Tramper J (1992) Effect of serum concentration on hybridoma viable cell density and production of monoclonal antibodies in CSTRs and on shear sensitivity in air-lift loop reactors. Biotechnol Bioeng 39, 891–897.

Martens DE, Gooijer CD de, Velden-de Groot CAM, van der Beuvery EC and Tramper J (1993) Effect of dilution rate on growth, productivity, cell cycle and size, and shear sensitivity of a hybridoma cell in a continuous culture. Biotechnol Bioeng 41, 429–439.

Michaels JD, Petersen JF, McIntire LV and Papoutsakis ET (1991) Protection mechanisms of freely suspended animal cells (CRL 8018) from fluid-mechanical injury. Viscometric and bioreactor studies using serum, pluronic F68 and polyethylene glycol. Biotechnol Bioeng 38, 169–180.

Mukhopadhyay A, Mukhopadhyay SN and Talwar GP (1993) Cellular affinity is the only deciding factor for microcarrier selection for the cultivation of anchorage dependent cells. Biotechnol techn 7, 173–176.

Murhammer DW and Goochee CF 61990) Sparged animal cell bioreactors: Mechanism of cell damage and pluronic F-68 protection. Biotechnol prog 6, 391–397.

Nikolai T and Hu W-S (1992) Cultivation of mammalian cells on macroporous microcarriers. Enzyme Microb technol 14, 203–213.

Nollert MU, Diamond SL and McIntire LV (1991) Hydrodynamic shear stress and mass transport modulation of endothelial cell metabolism. Biotechnol Bioeng 38, 588–602.

O'Connor KC, Papoutsakis ET (1992) Agitation effects on microcarrier and suspension CHO cells. Biotechnol Techn 6, 323–328.

Papoutsakis ET (1991) Fluid mechanical damage of animal cells in bioreactors. TibTech 9, 427–437.

Petersen JF, McIntire LV and Papoutsakis ET (1988) Shear sensitivity of cultured hybridoma cells (CRL-81018) depends on mode of growth, culture age and metabolic concentrations. J Biotechnol 7, 229–246.

Pol L van der, Zijlstra G, Thalen M and Tramper J (1990) Effect of serum concentration on production of monoclonal antibodies and on shear sensitivity of a hybridoma. Bioproc Eng 5, 241–245.

Pol L van der, Bonarius D, Wouw G van de and Tramper J (1993) Effect of silicone antifoam on shear sensitivity of hybridoma cells in sparged cultures. Biotechnol Prog 9, 504–509.

Riet K van 't and Tramper J (1991) Basic bioreactor design. Marcel Dekker Inc., New York.

Shiragami N, Honda H and Unno H (1993) Anchorage dependent animal cell culture using a porous microcarrier. Bioproc Eng 8, 295–299.

Tramper J, Williams JB, Joustra D (1986) Shear sensitivity of insect cells in suspension. Enzyme Microbiol Technol 8, 33–36.

Tramper J, Smit D, Straatman J and Vlak JM (1988) Bubble column design for growth of fragile insect cells. Bioproc Eng 3, 37–41.

Trinh K, Garcia-Briones M and Chalmers JJ (1994) Quantification of damage to suspended insect cells as a result of bubble rupture. Biotechnol Bioeng 43, 37–45.

Address for correspondence: D.E. Martens, Department of Food Science, Food and Bioengeneering Group, Agricultural University, Bomenweg 2, 6703 HD Wageningen, The Netherlands.